JACS
JOURNAL OF THE AMERICAN CHEMICAL SOCIETY
Communication
pubs.acs.org/JACS

Self-Assembly of Broadband White-Light Emitters

Emma R. Dohner,[†] Eric T. Hoke,[‡] and Hemamala I. Karunadasa*[,†]

[†]Department of Chemistry and [‡]Geballe Laboratory for Advanced Materials, Stanford University, Stanford, California 94305, United States

Supporting Information

ABSTRACT: We use organic cations to template the solution-state assembly of corrugated lead halide layers in bulk crystalline materials. These layered hybrids emit radiation across the entire visible spectrum upon ultraviolet excitation. They are promising as single-source white-light phosphors for use with ultraviolet light-emitting diodes in solid-state lighting devices. The broadband emission provides high color rendition and the chromaticity coordinates of the emission can be tuned through halide substitution. We have isolated materials that emit the "warm" white light sought for many indoor lighting applications as well as "cold" white light that approximates the visible region of the solar spectrum. Material syntheses are inexpensive and scalable and binding agents are not required for film deposition, eliminating problems of binder photodegradation. These well-defined and tunable structures provide a flexible platform for studying the rare phenomenon of intrinsic broadband emission from bulk materials.

Solid-state lighting (SSL) is an attractive solution to the inefficiencies of traditional incandescent and fluorescent lighting sources.[1] Artificial lighting constitutes ~20% of global electricity consumption. The transition to SSL devices has been projected to halve this value by the year 2025.[1] To mimic the blackbody radiation of an incandescent bulb, typical SSL devices consist of light-emitting diodes (LEDs) coated with a single phosphor (e.g., a blue LED coated with a yellow phosphor)[2] or a mixture of phosphors (e.g., an ultraviolet LED coated with red, green, and blue phosphors).[3] Both these strategies have drawbacks. Mixing phosphors results in efficiency losses due to self-absorption, and the different degradation rates of the individual phosphors lead to changes in emission color over time.[3] Single-phosphor-coated LEDs emit white light with poor color rendition due to discontinuities in the phosphor's emission.[3] To circumvent these problems, a major target in SSL research is a single-source broadband white-light-emitting phosphor.

Here, we report on solution-state synthetic routes to well-defined and single-phase white-light emitters (Figure 1). Broadband emission across the entire visible spectrum arises from corrugated lead halide sheets in a two-dimensional organic–inorganic perovskite. The emission can be tuned through halide substitution to afford both "warm" and "cold' white light. These hybrid perovskites are wide-bandgap semiconductors. The organic and inorganic components—layered at the angstrom scale—lead to electronic structures similar to those of nanostructures terminated by wide-bandgap capping groups. Therefore, these hybrids provide access to the exotic electronic properties of quantum-confined systems, but in bulk crystalline materials.[4] Unlike many nanoscale structures that have significant size distribution and can require specialized processing techniques, these materials are formed in solution using benchtop self-assembly reactions. The thickness of the inorganic layers is determined by the crystal structure and shows no size distribution between syntheses.

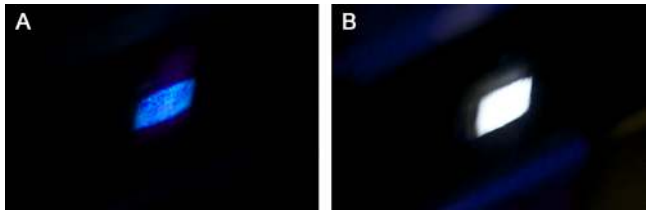

Figure 1. Photographs showing luminescence from powders of (A) (*N*-MPDA)[$PbBr_4$] (**1**) and (B) (*N*-MEDA)[$PbBr_4$] (**2**) under 380-nm irradiation.

The inorganic sheets of layered perovskites can be derived from the three-dimensional perovskite structure by slicing along specific crystallographic planes (e.g., (001) or (110)) (Figure 2). The vast majority of two-dimensional perovskites (more than 250 are reported in the Cambridge Structural Database) contain (001) layers, and we are aware of only three reports of structures with (110) layers.[5] We used two similar organic cations, N^1-methylethane-1,2-diammonium (*N*-MEDA) and N^1-methylpropane-1,3-diammonium (*N*-MPDA), to direct the solution-state assembly of (110) and (001) perovskites, respectively. We reasoned that the short length of *N*-MEDA would not allow for the formation of a (001) perovskite, as it would bring adjacent inorganic sheets too close together (Figure S1). As a dication, *N*-MEDA also cannot occupy the A^1-site of a three-dimensional perovskite. Due to the corrugated nature of the (110) sheets, the primary ammonium group of *N*-MEDA can form hydrogen bonds with halides from two adjacent inorganic sheets, likely stabilizing the (110) structure (Figures 2B and S2). In contrast, the longer *N*-MPDA cations can adequately separate (001) inorganic sheets, avoiding close contact between adjacent layers. The longer chain length would also not allow for hydrogen bonds between the ammonium groups and adjacent inorganic sheets in the (110) perovskite structure. Consistent with these arguments, *N*-MPDA forms the (001) perovskite (Figure 2A).

Received: October 29, 2013
Published: January 14, 2014

dx.doi.org/10.1021/ja411045r | *J. Am. Chem. Soc.* 2014, 136, 1718–1721

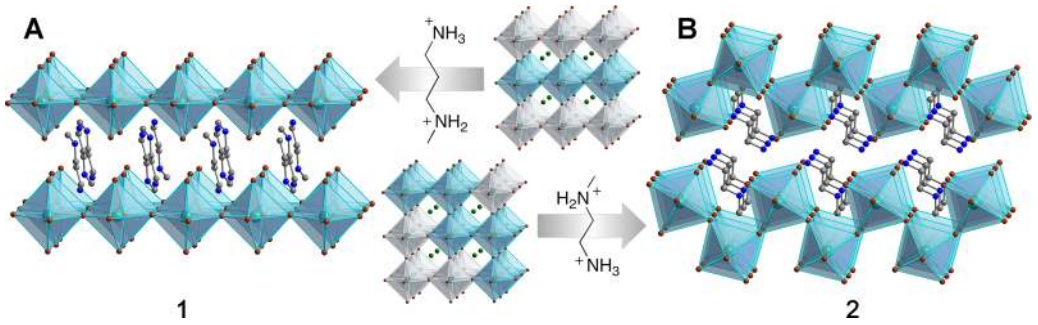

Figure 2. X-ray structures of (A) the (001) perovskite (*N*-MPDA)[$PbBr_4$] (**1**, *N*-MPDA = N^1-methylpropane-1,3-diammonium) and (B) the (110) perovskite (*N*-MEDA)[$PbBr_4$] (**2**, *N*-MEDA = N^1-methylethane-1,2-diammonium). The center panel shows the three-dimensional perovskite ($MeNH_3$)[$PbBr_3$] with the (001) (top) and (110) (bottom) planes shaded in turquoise. Turquoise, brown, blue, and gray spheres represent Pb, Br, N, and C atoms, respectively. Green spheres represent $MeNH_3^+$. H and disordered atoms in the organic groups are omitted for clarity.

The absorption spectrum of (*N*-MPDA)[$PbBr_4$] (**1**) is similar to those of other reported (001) lead bromide perovskites with a sharp excitonic absorption at 420 nm, characteristic of dimensionally reduced inorganic structures,[6] and a bandgap of ~350 nm (3.5 eV) (Figure 3A). Upon excitation at 410 nm, the emission spectrum shows a sharp peak at 433 nm with a full width at half-maximum (fwhm) of 24 nm. The absorption spectrum of (*N*-MEDA)[$PbBr_4$] (**2**) shows a similarly sharp exciton band at 395 nm with a shoulder at 370 nm (Figure 3B). The bandgap of ~330 nm (3.8 eV) is higher than that for **1**, consistent with the greater electronic confinement of the corrugated sheets. Interestingly, despite the similarity of the absorption spectra, the photoluminescence behavior of **2** is dramatically different from that of **1**. Upon 380-nm excitation, **2** shows a broad emission that spans the entire visible spectrum (Figure 3B). The higher-energy shoulder peaks at ~420 nm, and the lower-energy band is broader and more intense with a maximum at 558 nm and a fwhm of 165 nm. The very large Stokes shift of 170 nm for the 558-nm emission leads to low self-absorption. Two-dimensional excitation−emission spectra (Figure S6) show that both the 420- and 550-nm emissions originate from the same excitation features at 368 and 393 nm. These materials can therefore be excited at wavelengths corresponding to the highest reported quantum efficiencies of current LEDs (380−410 nm).[3b]

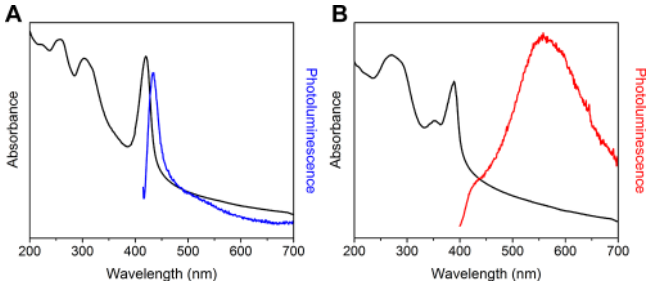

Figure 3. (A) Absorption spectrum (black) and emission spectrum (blue, excitation at 400 nm) for (*N*-MPDA)[$PbBr_4$] (**1**). (B) absorption spectrum (black) and emission spectrum (red, excitation at 380 nm) for (*N*-MEDA)[$PbBr_4$] (**2**).

Unlike phosphors used in many fluorescent lamps and commercial SSL devices, **2** has significant emission intensity in the red region of the visible spectrum. As a consequence, the emission lies to the yellow side of pure white light with chromaticity coordinates (CIE)[3a] of (0.36, 0.41) and a correlated color temperature (CCT) of 4669 K, resulting in the "warm" white light sought for many indoor lighting applications. In order to tune the chromaticity of the emission, we then synthesized a family of mixed-halide perovskites. Emission tunability is important when implementing SSL in applications such as navigation lights for airplanes and military signs, where lighting specifications must match previously defined values.[3b] Conducting the assembly reactions in a mixture of 9 M HBr and 12 M HCl afforded the series (*N*-MEDA)[$PbBr_{4-x}Cl_x$] (x = 0−1.2), where x was determined through inductively coupled plasma analysis. Powder X-ray diffraction (XRD) patterns indicate the formation of single-phase crystalline materials, with a systematic shift to smaller lattice spacings upon exchange of bromide for chloride ions (Figure S8). Emission spectra of the mixed-halide perovskites show a systematic blue-shift with increasing chloride content, with the trend especially prominent in the higher energy shoulder (Figure S9). The x = 0.5 member of the series comes closest to pure-white light (CIE coordinates of (0.33,0.33)), with CIE coordinates of (0.31,0.36) and a CCT of 6502 K, resulting in "cold" white light. Chloride substitution also improves the material's color rendering index (CRI), which is a measure of how accurately illuminated colors are reproduced compared with a blackbody light source. While **2** has a CRI of 82, (*N*-MEDA)[$PbBr_{3.5}Cl_{0.5}$] has a CRI of 85. These are well above the values for basic fluorescent light sources (~65) and approach the high CRI indexes (>90) of mixed-phosphor light sources, but in single-phase materials.[3a]

We used a reported procedure[7] to measure the photoluminescence quantum efficiency (PLQE) of the broad emission of **2** (from 400 to 700 nm) to be ~0.5%. This efficiency can be improved by chloride substitution, with (*N*-MEDA)[$PbBr_{2.8}Cl_{1.2}$] exhibiting a PLQE of 1.5%. These values are comparable to the original PLQEs of 2−3% reported for CdSe nanocrystals in colloidal suspensions.[8] PLQEs for these white-light-emitting nanocrystals have been substantially increased to 10−45% through the use of capping groups[9] and dopants,[10] albeit with a shift in CIE coordinates.[11] Luminescence from CdSe nanocrystals is readily quenched through particle aggregation,[12] and their application in SSL will require a dispersive polymer that is resistant to photodegradation by the ultraviolet LED.[9a] Because **2** is assembled in solution at room temperature, films can be easily deposited on substrates, using inexpensive methods such as drop casting and spin coating, without requiring binding agents. To assess long-term performance, we then continuously irradiated **2** for seven days in an evacuated quartz ampule with a 365-nm 4-W lamp. We did not observe any material degradation or decrease in

dx.doi.org/10.1021/ja411045r | J. Am. Chem. Soc. 2014, 136, 1718−1721

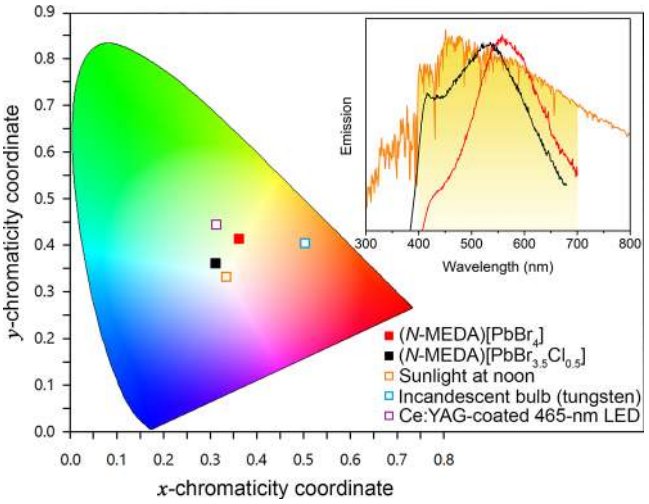

Figure 4. Chromaticity coordinates (CIE) of white-light emitters. Inset: Solar spectrum (orange) with the visible region shaded in yellow and emission spectra of (*N*-MEDA)[$PbBr_4$] (**2**, red, excited at 380 nm) and (*N*-MEDA)[$PbBr_{3.5}Cl_{0.5}$] (black, excited at 360 nm). CIE coordinates for the Ce:YAG-coated blue LED were obtained from ref 22.

photoluminescence during this period—PLQE values obtained before and after the experiment were within experimental error.

Broadband emission from nanometer-scale CdSe crystals has been attributed to mid-bandgap states arising from deep traps at surface sites.[8] Indeed, this emission becomes more pronounced as higher surface area to volume ratios are reached with decreasing particle size.[13] All optical measurements of (*N*-MEDA)[$PbBr_{4-x}Cl_x$] were conducted on powders with particles sizes greater than 10 μm, and we see similar emission spectra from drop-cast polycrystalline films and ball-milled powder (Figure S10). This indicates that the emission is likely a property of the bulk material.

To probe the origin of the broad emission in **2**, we obtained time-resolved photoluminescence measurements using a pulsed-laser diode with an excitation wavelength of 375 nm. The lifetime of the emission from **2** is constant over the full range from 400 to 700 nm, indicating an origin from similar excited states (Figure S11). A fit to the initial 2 ns of data gives a lifetime of 1.2 ns for **2**, longer than the pico-second lifetimes reported for lead iodide (001) perovskites.[14] For comparison, emission from the (001) perovskite **1** has a lifetime of 0.38 ns. We hypothesize that the emission from **2** arises from excitons trapped through elastic lattice deformations. Strong vibronic coupling between excitons and the lattice can cause broadband emission due to an excited state that is highly distorted with respect to the ground state. The corrugated sheets of **2** may allow for greater lattice distortion and stronger electron–nuclear coupling compared to the inorganic layers in **1**. Luminescence from radiative decay of such "self-trapped" excitons has been previously studied in (001) lead halide perovskites,[15] alkali halide crystals,[16] organic molecular crystals,[17] and platinum chain compounds.[18]

Due to the complexity of rigorously size-selective quantum dot syntheses, bulk white-light emitting materials synthesized by solvothermal or solution-state reactions are especially attractive. However, reports of single-phase bulk white-light emitters are scarce. Recently, white-light emission has been reported in the layered material Cd_2E_2(alkylamine) (E = S, Se, and Te), which is prepared via solvothermal routes.[19] The PLQEs of the original materials (4–5%) have been improved up to 37% using a combination of metal and chalcogen substitution, Mn^{2+}-doping, and crystal engineering. To the best of our knowledge, white-light emission from layered perovskites has not been reported. A broad yellow emission in the (110) perovskite (1-(3-ammoniopropyl)-1*H*-imidazol-3-ium)[$PbBr_4$] has been attributed to energy transfer from the inorganic sheets to photoactive molecules in the organic layers.[5c] Based on our results, however, this emission may be solely due to the inorganic sheets. The analogous three-dimensional perovskites (CH_3NH_3)[PbX_3] (X = Cl, Br, or I), which have much lower exciton binding energies, have recently been employed as absorbers in solar cells with efficiencies of up to 15%.[20]

These first-generation materials have impressive tunability of CIE coordinates, high CRI values, sustained activity under continuous illumination, inexpensive and scalable syntheses, and binder-free film deposition methods. Current SSL devices use phosphors consisting of metal oxide or metal nitride hosts with rare-earth dopants such as Eu^{3+} or Ce^{3+}, which require high-temperature solid-state syntheses (1300–1900 °C).[3] These hybrid perovskites are synthesized at room temperature and are stable up to decomposition temperatures of 250 °C (Figure S12). Lead is also less toxic than mercury currently used in fluorescent lamps and cadmium found in developing SSL technologies.[21] However, for these materials to be viable alternatives to commercial phosphors, their quantum efficiencies must be increased. Our efforts are focused on improving these values using methods such as further separating the inorganic layers with longer organic cations, substituting inorganic ions, and incorporating luminescent centers (e.g., Mn^{2+}). Our ongoing studies are probing the emission mechanism using band-structure calculations, vibrational spectroscopy, and temperature-dependent photoluminescence spectroscopy, to find general design principles for the assembly of intrinsic white-light emitters.

■ ASSOCIATED CONTENT

Supporting Information

Experimental details, spectra, and crystallographic data. This material is available free of charge via the Internet at http://pubs.acs.org. The CIF files for **1** and **2** have been deposited in the Cambridge Crystallographic Data Centre under deposition numbers CCDC 961380 and 961379, respectively.

■ AUTHOR INFORMATION

Corresponding Author

hemamala@stanford.edu

Notes

The authors declare no competing financial interest.

■ ACKNOWLEDGMENTS

We thank Stanford University for start-up funds and support for E.R.D. through the Bing Summer Undergraduate Research Program and the Undergraduate Advising and Research Major Grant. Single-crystal and powder XRD studies were performed at the Stanford Nanocharacterization Laboratory, part of the Stanford Nano Shared Facilities. We thank Dr. D. Solis-Ibarra for assistance with crystallography, Profs. D. R. Gamelin and E. I. Solomon for valuable discussions, and Prof. M. D. McGehee for providing generous access to equipment.

REFERENCES

(1) (a) U.S. Department of Energy and Optoelectronics Industry Development Association. *The Promise of Solid State Lighting for General Illumination*; Optoelectronics Industry Development Association: Washington DC, 2002. (b) Sandia National Laboratories. Solid-State Lighting Science EFRC, http://energy.sandia.gov/?page_id=452 (accessed Nov 2013).

(2) (a) Wu, J. L.; Gundiah, G.; Cheetham, A. K. *Chem. Phys. Lett.* **2007**, *441*, 250. (b) Im, W. B.; George, N.; Kurzman, J.; Brinkley, S.; Mikhailovsky, A.; Hu, J.; Chmelka, B. F.; DenBaars, S. P.; Seshadri, R. *Adv. Mater.* **2011**, *23*, 2300.

(3) (a) Ye, S.; Xiao, F.; Pan, Y. X.; Ma, Y. Y.; Zhang, Q. Y. *Mater. Sci. Eng., R* **2010**, *71*, 1. (b) Silver, J.; Withnall, R. In *Luminescent Materials*, Kitai, A., Ed.; John Wiley & Sons: Chichester, 2008; p 75.

(4) (a) Mitzi, D. B. *Prog. Inorg. Chem.* **1999**, *48*, 1. (b) Mitzi, D. B. *J. Chem. Soc., Dalton Trans.* **2001**, 1.

(5) (a) Mitzi, D. B.; Wang, S.; Feild, C. A.; Chess, C. A.; Guloy, A. M. *Science* **1995**, *267*, 1473. (b) Li, Y.; Zheng, G.; Lin, J. *Eur. J. Inorg. Chem.* **2008**, 1689. (c) Li, Y. Y.; Lin, C. K.; Zheng, G. L.; Cheng, Z. Y.; You, H.; Wang, W. D.; Lin, J. *Chem. Mater.* **2006**, *18*, 3463.

(6) (a) Takeoka, Y.; Asai, K.; Rikukawa, M.; Sanui, K. *Bull. Chem. Soc. Jpn.* **2006**, *79*, 1607. (b) Cheng, Z.; Lin, J. *CrystEngComm* **2010**, *12*, 2646.

(7) de Mello, J. C.; Wittmann, H. F.; Friend, R. H. *Adv. Mater.* **1997**, *9*, 230.

(8) Bowers, M. J.; McBride, J. R.; Rosenthal, S. J. *J. Am. Chem. Soc.* **2005**, *127*, 15378.

(9) (a) McBride, J. R.; Dukes, A. D.; Schreuder, M. A.; Rosenthal, S. J. *Chem. Phys. Lett.* **2010**, *498*, 1. (b) Schreuder, M. A.; McBride, J. R.; Dukes, A. D.; Sammons, J. A.; Rosenthal, S. J. *J. Phys. Chem. C* **2009**, *113*, 8169. (c) Sapra, S.; Mayilo, S.; Klar, T. A.; Rogach, A. L.; Feldmann, J. *Adv. Mater.* **2007**, *19*, 569.

(10) Shen, C.-C.; Tseng, W.-L. *Inorg. Chem.* **2009**, *48*, 8689.

(11) Rosson, T. E.; Claiborne, S. M.; McBride, J. R.; Stratton, B. S.; Rosenthal, S. J. *J. Am. Chem. Soc.* **2012**, *134*, 8006.

(12) Noh, M.; Kim, T.; Lee, H.; Kim, C.-K.; Joo, S.-W.; Lee, K. *Colloids Surf., A* **2010**, *359*, 39.

(13) Landes, C. F.; Braun, M.; El-Sayed, M. A. *J. Phys. Chem. B* **2001**, *105*, 10554.

(14) Fujita, T.; Nakashima, H.; Hirasawa, M.; Ishihara, T. *J. Lumin.* **2000**, *87*−*89*, 847.

(15) (a) Kitazawa, N.; Aono, M.; Watanabe, Y. *Mater. Chem. Phys.* **2012**, *134*, 875. (b) Kitazawa, N.; Ito, T.; Sakasegawa, D.; Watanabe, Y. *Thin Solid Films* **2006**, *500*, 133.

(16) Castner, T. G.; Känzig, W. *J. Phys. Chem. Solids* **1957**, *3*, 178.

(17) Matsui, A.; Mizuno, K.-i.; Tamai, N.; Yamazaki, I. *Chem. Phys.* **1987**, *113*, 111.

(18) (a) Rössler, U.; Yersin, H. *Phys. Rev. B* **1982**, *26*, 3187. (b) Tomimoto, S.; Nansei, H.; Saito, S.; Suemoto, T.; Takeda, J.; Kurita, S. *Phys. Rev. Lett.* **1998**, *81*, 417.

(19) (a) Ki, W.; Li, J. *J. Am. Chem. Soc.* **2008**, *130*, 8114. (b) Ki, W.; Li, J.; Eda, G.; Chhowalla, M. *J. Mater. Chem.* **2010**, *20*, 10676. (c) Roushan, M.; Zhang, X.; Li, J. *Angew. Chem., Int. Ed.* **2012**, *51*, 436.

(20) (a) Kojima, A.; Teshima, K.; Shirai, Y.; Miyasaka, T. *J. Am. Chem. Soc.* **2009**, *131*, 6050. (b) Liu, M.; Johnston, M. B.; Snaith, H. J. *Nature* **2013**, *501*, 395. (c) Burschka, J.; Pellet, N.; Moon, S.-J.; Humphry-Baker, R.; Gao, P.; Nazeeruddin, M. K.; Gratzel, M. *Nature* **2013**, *499*, 316.

(21) Alloway, B. J.; Ayres, D. C. *Chemical Principles of Environmental Pollution*, 3rd ed.; Chapman & Hall: London, UK, 1997; p 208.

(22) Nishiura, S.; Tanabe, S.; Fujioka, K.; Fujimoto, Y.; Nakatsuka, M. Preparation and optical properties of transparent Ce:YAG ceramics for high power white LED. IUMRS-ICA 2008 Symposium, 9−13 Dec 2008, Nagoya, Japan; IOP Conference Series: Materials Science and Engineering; IOP Publishing: Bristol, UK, 2009; Vol. *1*, 012031.